

Specific intermediate-valence state of insulating $4f$ compounds detected by L_3 x-ray absorption

A. Bianconi and A. Marcelli

Dipartimento di Fisica, Università degli Studi di Roma "La Sapienza," I-00185 Roma, Italy

H. Dexpert and R. Karnatak

Laboratoire de l'Utilisation du Rayonnement Electromagnétique (LURE), Université de Paris—Sud, F-91405 Orsay, France

A. Kotani and T. Jo

Department of Physics, Faculty of Science, Osaka University, Toyonaka, Osaka 560, Japan

J. Petiau

Laboratoire de Minéralogie-Cristallographie, Université de Paris VI et Université de Paris VII, F-75230 Paris, France

(Received 4 September 1985; revised manuscript received 2 July 1986)

The intermediate valence of formally tetravalent compounds has been detected by L_3 x-ray-absorption near-edge structure (XANES) in CeO_2 and in PrO_2 but not in UO_2 , which have the same CaF_2 structure and large f and ligand mixing. The intermediate valence has been found both in CeO_2 and in $\text{Ce}(\text{SO}_4)_2 \cdot 4\text{H}_2\text{O}$, which have similar local structure but different crystal structure. We show that L_3 XANES final states are a direct probe of configuration interaction between $4f^n$ and $4f^{n+1}\underline{L}$ configurations in the ground state and that the weight of the $4f^{n+1}\underline{L}$ in the ground state can be deduced. The many-body final states arise from the characteristic properties of these materials: (i) the presence of localized $4f$ level above the oxygen $2p$ band separated by a gap $\delta\epsilon$ with relevant correlation energy U_{ff} ($U_{ff} \geq \delta\epsilon$) and (ii) mixing of $4f$ localized states with ligand valence orbitals such that the hybridization energy V is of the same order of magnitude as the energy separation ΔE between the many-body configuration $4f^n$ and $4f^{n+1}\underline{L}$ ($V \geq \Delta E$). These insulating materials, which cannot be classified as standard mixed-valence systems, are called here interatomic intermediate-valence systems.

I. INTRODUCTION

The unexpected presence of mixed-valence behavior in hard spectroscopies, like x-ray photoemission spectroscopy (XPS) and in x-ray-absorption near-edge structure (XANES), of an insulating $4f$ compound like CeO_2 (Refs. 1–6) and more recently also in Sm in an argon matrix⁷ and in EuO under high pressure⁸ has attracted a great amount of interest. A controversy has arisen between the proposed mixed-valence state of insulating CeO_2 in the ground state⁴ and the role of final-state effects.^{3,5} On the other hand, a controversy has arisen on the interpretation of the data in terms of a many-body configuration theory for a local cluster (CeO_8), predicting configuration interaction in the ground state,^{9,10} or in terms of one-electron band structure of the crystal.¹¹

According to the table of transition metals proposed by Smith and Riseborough,¹² there is a crossover region of materials going from cerium through palladium between the regions where the d and f electrons are localized and where they are itinerant. Here we have investigated Ce, Pr, and U compounds which belong to this crossover region. In UO_2 , PrO_2 , and CeO_2 , with CaF_2 crystal structure and eightfold metal coordination, evidence of large mixing of metal f and oxygen $2p$ orbitals has been found both from band-structure¹³ and molecular-orbital calculations for CeO_8 (Ref. 14) and UO_8 (Ref. 15) clusters.

The Ce L_3 XANES spectrum of CeO_2 remained an un-

solved puzzle for many years since the first experiment.^{1,3–6} In fact, the L_3 XANES of transition metals, actinides, and lanthanides exhibit a single white line at threshold which is due to a resonance in the $2p \rightarrow 5d$ cross section modified by local density of unoccupied states. This resonance can be obtained by one-electron theories¹⁶ both using multiple-scattering approach of XANES in the real space¹⁷ as well as in the k space in the frame of band-structure approach.¹⁸ On the contrary, the spectrum of CeO_2 shows two well-resolved white lines like the spectra of mixed-valence Ce intermetallics. But the energy separation of only 7 eV between $4f^1$ and $4f^0$ configurations (to be compared with 11 eV in intermetallics) remained unexplained as pointed out in Ref. 5.

In this experiment we have measured the spectra of a set of systems with similar local structure MO_8 ($M = \text{Ce}, \text{Pr}, \text{and U}$), and therefore with similar one-electron absorption cross sections. The one-electron cross section has been obtained from the spectrum of UO_2 and the many-body effects in the other compounds have been determined experimentally.

We interpret the data by a many-body calculation of the oscillator strength of the core $2p \rightarrow 5d$ excitations in the x-ray absorption which predicts the splitting of the white line and the line shape of experimental features in the cases where the many-body description in the framework of the theory of configuration interaction of the ground state of insulating oxides is required.

This theory allows us to obtain a picture of configuration interaction for a local cluster model as well as for the band-structure limit. The band structure effects are predicted by the theory and verified experimentally by comparison between the spectra of CeO_2 and cerium sulfate. The value of the Coulomb interaction $U_{df}=5$ eV between the $5d$ photoelectron and the $4f$ electron has been found in CeO_2 and it plays a key role in XANES.

This work shows that there is a set of systems: CeO_2 , cerium sulfate and PrO_2 , which show configurations interaction in the ground state. In these systems the correlation energy U_{ff} is not negligible and at the same time the hybridization between the two configurations V is of the order of magnitude as their energy separation ΔE . We call these systems interatomic intermediate-valence (IIV) insulating systems to be distinguished from the metallic mixed-valence systems, which, as defined by Varma,¹⁹ show the spectral weight of the $4f$ states in a single peak of the density of states at the Fermi level. In the one-electron language the $4f$ weight in insulating IIV systems is distributed between occupied and unoccupied states separated by the energy gap because of large hybridization between f and ligand orbitals.

EXPERIMENT

The experiment has been performed on well-characterized stoichiometric samples both at Frascati synchrotron radiation facility and in LURE at Université Paris Sud. Experimental details have been described elsewhere.^{20,21}

RESULTS AND DISCUSSION

In Fig. 1 we report the L_3 XANES spectra of UO_2 , PrO_2 , CeO_2 , and $\text{Ce}(\text{SO}_4)_2 \cdot 4\text{H}_2\text{O}$. The zero of the energy scale of UO_2 has been fixed at the white line maximum and the other spectra have been aligned to superimpose the EXAFS oscillations and the XANES multiple-scattering feature at about 40 eV in Fig. 1. UO_2 , PrO_2 , and CeO_2 have the same crystal structure and similar one-electron band structure.^{13,22} In fact, the valence-band photoemission and BIS spectra of UO_2 and CeO_2 show many similarities.^{11,23} We have found that the gross features of EXAFS and XANES above the white line are similar. The discussion of subtle differences between XANES and EXAFS spectra of these systems will be discussed in a forthcoming paper. The main differences between the spectra in Fig. 1 appear at threshold.

In Fig. 2 we report the spectra of CeO_2 and cerium sulfate which have similar cerium oxygen distance and the same site geometry as shown by EXAFS and XANES spectra. The large variation of intensities and line shapes of the peaks *A* and *B* appears clearly.

The UO_2 spectrum shows at threshold a single white line due to a core transition to the unoccupied U $6d$ orbitals enhanced by the resonance in the atomic absorption cross section for $2p \rightarrow 6d$ transitions.

We have measured also the M_3 absorption spectrum of UO_2 where the core hole lifetime is different and experimental resolution is better, and we have found a similar single white line. The one-electron XANES multiple-

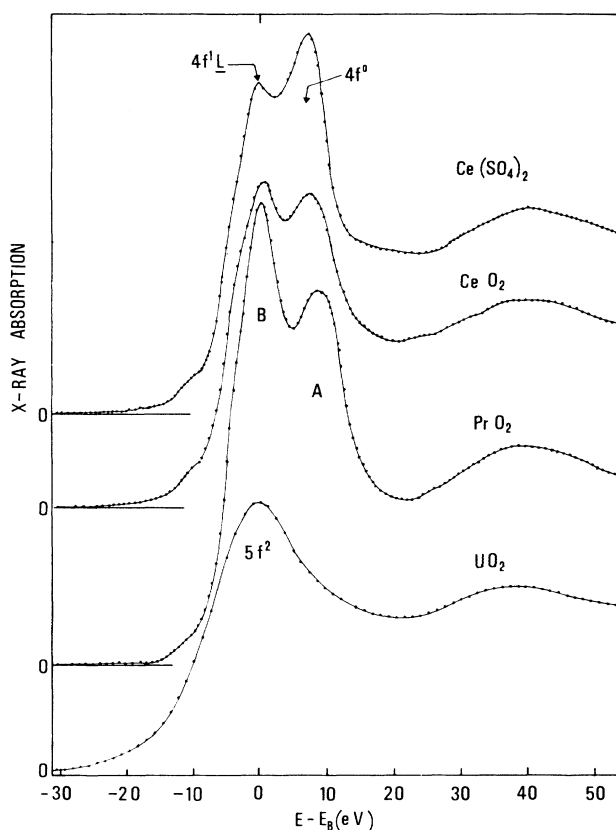


FIG. 1. XANES spectra of $\text{Ce}(\text{SO}_4)_2 + 4\text{H}_2\text{O}$, CeO_2 , PrO_2 , and UO_2 at the metal L_3 threshold. The spectra have been aligned to overlap the high-energy XANES and EXAFS features. The zero of the energy scale is fixed at the first main absorption feature.

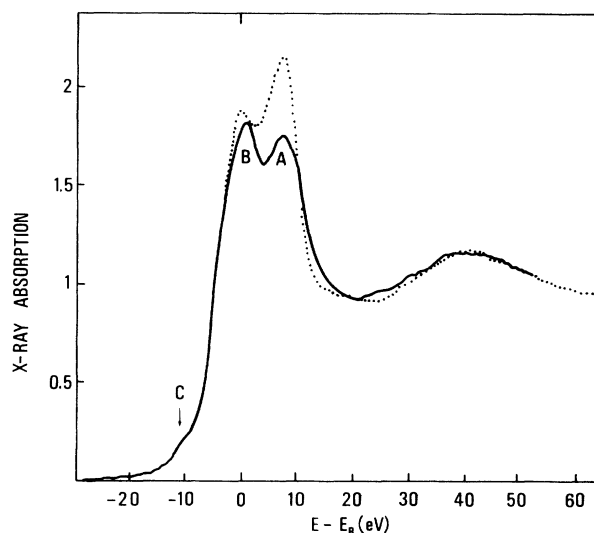


FIG. 2. L_3 absorption spectra of cerium in CeO_2 (solid line) and $\text{Ce}(\text{SO}_4)_2 + 4\text{H}_2\text{O}$ (dotted line).

scattering theory for a small cluster ErO_6 including only the nearest neighbors¹⁷ gives an account of the $2p \rightarrow 5d$ white line at threshold and for the main multiple-scattering MS resonance at about 40 eV. Because all other samples have the same local structure we expect similar one-electron multiple-scattering XANES resonance.¹⁶ The L_3 spectrum of CeO_2 in Fig. 1 shows two well-known white lines in agreement with previous works.¹⁻⁵ The comparison between the L_3 spectra of UO_2 and CeO_2 shows that the peak *B* of CeO_2 spectrum is the fully screened configuration of valence electrons which is the static single configuration of the one-electron model for core transitions.¹⁶ The presence of two white lines shows the breakdown of the one-electron description for core transition in these systems. The different peaks correspond to different final-state configurations with different configurations of valence electrons.

These many-body features in the final state can be determined by configuration interaction in the final state induced by the relaxation effects around the core hole and/or by configuration interaction in the initial state when correlation effects are important.

Final-state satellites in XANES are very weak when compared with x-ray photoelectron spectroscopy (XPS). This has been shown experimentally^{6,20,24} and it can be demonstrated in the frame of the many-body theory presented below.

We will show that the many-body features in the XANES of tetravalent Ce compounds are determined by the configuration interaction mainly in the initial state. The electronic structure of correlated systems where there is a large mixing between localized $4f$ levels and more delocalized ligand (O $2p$ in our case) levels can be described by mixing of localized ionic multielectron configurations: $4f^0$ and $4f^1\bar{L}$, where \bar{L} denotes a ligand hole. The ground state is described by the wave function $\Psi_g = a |4f^0\rangle + b |4f^1\bar{L}\rangle$. The two ionic configurations before hybridization are separated by ΔE . The hybridization energy V between the atomlike localized $4f$ and delocalized O $2p$ states determines the mixing between the multielectron configurations. Here we extend the meaning of the notation \bar{L} , introduced by Fujimori⁹ for a hole in the molecular O $2p$ states of the CeO_8 cluster, to a hole in O $2p$ band of a crystal with large dispersion. Finally the electronic Coulomb repulsion U_{ff} describes the correlation of localized f states.

Now we discuss the final states at threshold of L_3 XANES for IIV systems. In the final state, at the white line maxima, a core hole is in the metal atom and a photoelectron is excited at the first $5d$ unoccupied band. The final state is determined by the Coulomb interactions Q_{hd} between the $5d$ electron and the core hole, and Q_{hf} between the f electrons and the core hole, and the Coulomb repulsion U_{df} between the $5d$ and f electrons. As first pointed out by Kotani and Toyozawa²⁵ because of the large Q_{hf} interaction the f states are deepened by the core hole, as in XPS but because the Coulomb repulsion U_{df} the f levels are pushed up in the x-ray absorption. This last effect is absent in XPS, i.e., $U_{df}=0$, and therefore the XPS core final states are different from the XANES final states.^{6,26,27} This explains the fact that each core spectroscopy

gives different final states with different energy separation and mixing of final-state configurations. Therefore the intensity ratio between multielectron final states in XPS, $M_{4,5}$ XANES or $N_{4,5}$ XANES, are quite different and the deduction of ground-state intermediate valence requires a theoretical description of the final states.

The final states in XANES of IIV systems can be calculated, within the cluster model starting with a $4f$ level, a single ($N=1$) O $2p$ orbital with a mixing parameter V between them, and a single unoccupied $5d$ orbital. The eigenstate, with the lowest energy E_g which is assumed to be a singlet state, of the initial-state Hamiltonian is denoted by $|g\rangle$ and the L_3 absorption final state at energy E_f by $|f\rangle$. For details of these quantities we refer to Ref. 26. Then the L_3 edge spectrum $F_L(\omega)$ is expressed such that

$$F_L(\omega) = \sum_f |\langle f | a_d^\dagger a_c | g \rangle|^2 L(\omega + E_g - E_f), \quad (1)$$

where $L(x) = \Gamma / [\pi(x^2 + \Gamma^2)]$ and ω is the photon energy. Γ represents the spectral broadening due to finite lifetime of the core hole, a_d^\dagger denotes the creation operator of atomic Ce $5d$ orbital, and a_c expresses the annihilation of the core electron.

The band-structure effects determine an oxygen $2p$ bandwidth in MO_2 ($M = \text{Ce, Pr, and U}$), $W = 3$ eV.^{11,13,22,23} To take account of this effect in the calculations we treat the valence band with energy ε_k^v as a finite system consisting of N discrete levels given by

$$\varepsilon_k^v = -W/2 + (W/N)(k - \frac{1}{2}) \quad (k = 1, 2, \dots, N)$$

where W is the valence-band width and we put $W = 3$ eV; the center of the valence band is taken as the origin of energy. The Ce $5d$ band is similarly replaced by N discrete levels with the bandwidth 6 eV. Therefore the $N=1$ model is similar to the Fujimori cluster model (in the case of XPS) and by increasing N we obtain the band-structure model. With the fixed value of N , we have exactly diagonalized the model Hamiltonian of our Ce compounds,

$$\begin{aligned} H = & \sum_{\sigma', k} \varepsilon_k^v n_v(k, \sigma) + \sum_{\sigma} \varepsilon_f^0 n_f(\sigma) + \sum_k \varepsilon_k^d n_d(k) \\ & + \varepsilon_c n_c + (V/\sqrt{N}) \sum_{\sigma, k} [a_v^\dagger(k, \sigma) a_f(\sigma) + \text{h.c.}] \\ & + U_{ff} n_f(\uparrow) n_f(\downarrow) + (U_{df}/N) \sum_{\sigma, k, k'} n_f(\sigma) a_d^\dagger(k) a_d(k') \\ & + (1 - n_c) \left[Q_{hf} \sum_{\sigma} n_f(\sigma) + (Q_{hd}/N) \sum_{k, k'} a_d^\dagger(k) a_d(k') \right], \end{aligned} \quad (2)$$

where ε_k^v , ε_f^0 , ε_k^d , and ε_c are energies of the valence band, $4f$ level, $5d$ band, and core level, and $n_v(k, \sigma)$, $n_f(\sigma)$, $n_d(k)$, and n_c and their occupation number opera-

tors (the spin σ in the $5d$ and core states is disregarded). The operators $a_v^\dagger(k, \sigma)$ and $a_f(\sigma)$ represent the creation of the valence electron and the annihilation of the $4f$ electron, respectively, and $a_d^\dagger(k)$ and $a_d(k')$ represent the creation and annihilation of the $5d$ electron. For the method of diagonalizing H , we refer to Ref. 27. By using the ground state $|g\rangle$ of the Hamiltonian H with $n_c=1$ and the final state $|f\rangle$ of H with $n_c=0$, the absorption spectra $F_L(\omega)$ of Eq. (1) are calculated, and the calculated $F_L(\omega)$ for increasing values of N are found to converge for $N > 4$ and $\Gamma=1$ eV.

The energy separation between the $4f$ level ϵ_f^0 and the O $2p$ level (center of the O $2p$ valence band) is assumed to be $\delta\epsilon=1.6$ eV which in the many-body picture corresponds to the energy separation ΔE between $4f^0$ and $4f^1\bar{L}$ configurations. The values of $U_{ff}=10.5$ eV and $V=2.0$ eV (in agreement with finding from XPS core spectra)^{27,28} have been assumed to describe the ground state. These values of $\delta\epsilon$, V , and U_{ff} determine the interatomic intermediate valence in CeO_2 .

In the final state for the excitation of a $2p$ core hole and a $5d$ photoelectron we expect three configurations $4f^0$, $4f^1$, and $4f^2$. The energy separations are approximately given by

$$E(f^1) - E(f^0) = \delta\epsilon + Q_{hf} + U_{df}, \quad (3)$$

$$E(f^2) - E(f^0) = 2(\delta\epsilon + Q_{hf} + U_{df}) + U_{ff}. \quad (4)$$

We assign the many-body features B and A of CeO_2 in Fig. 1 to the $4f^1\bar{L}$ and the feature A to the $4f^0$ (mixed with $4f^2\bar{L}^2$) configurations, respectively. The interaction Q_{hf} plays a key role in the final states of XPS spectra of $3d$ core lines. Q_{hd} and U_{df} are essential to describe the L_3 XANES final states. Here the value of $Q_{hf} = -12.5$ eV was determined from $\text{Ce}(3d)$ XPS spectra as represented in Ref. 27. The two quantities Q_{hd} and U_{df} were obtained as -6 and 5 eV, respectively, to reproduce the energy separation and relative intensity of experimental peaks A and B in L_3 absorption spectra of CeO_2 . The results of the many-body calculations are plotted in Fig. 3 for the cluster model $N=1$ and for the band model $N=6$. The energy separation between peaks A and B in the calculation shown in Fig. 3 is in good agreement with the energy separations of the white lines in CeO_2 and cerium sulfate. Previous studies of L_3 XANES (Ref. 29) did not take account of the Coulomb interaction U_{df} and they obtained an energy separation of the white lines in disagreement with the experiment.

As found from Eq. (4), the $4f^2$ configuration in the final state is pushed at high energy by U_{ff} and $2u_{df}$ contributions therefore the low-energy feature B is mostly pure $4f^1$ and probes only the weight of the $|4f^1\bar{L}\rangle$ configuration in the ground state. On the contrary the $4f^0$ and $4f^2$ configurations are very close and mixed.

This is an important point that makes L_3 XANES and core-level XPS complementary methods for the determination of ground-state properties of IIV systems. In fact, in the final state of the $3d$ XPS spectroscopy of CeO_2 we have a different situation because the $4f^1$ is mixed with the $4f^2$ configuration and well separated from $4f^0$ configuration.

The finite bandwidth (see the difference between the $N=6$ and the $N=1$ spectrum) determines a broadening of the $4f^1$ (low-energy B feature) and the $4f^2$ final states. This effect is much larger for the $4f^2$ state which cannot be anymore identified as a sharp spectral feature in the band model calculation.

The line shape of white lines at threshold has been analyzed by a fitting procedure. We have subtracted from the L_3 absorption spectrum of UO_2 an arctangent curve to simulate the absorption jump from the pre-edge value to the atomic value of the absorption coefficient well above the edge $\mu_{a\infty}$. The residue of the subtraction is shown in Fig. 4. A good fit of the residue of the UO_2 spectrum by a single Lorentzian has been obtained as shown in Fig. 4. This peak is assigned to the single $5f^2$ configuration. The spectrum of UO_2 does not show many-body effects, and it looks like that of condensed

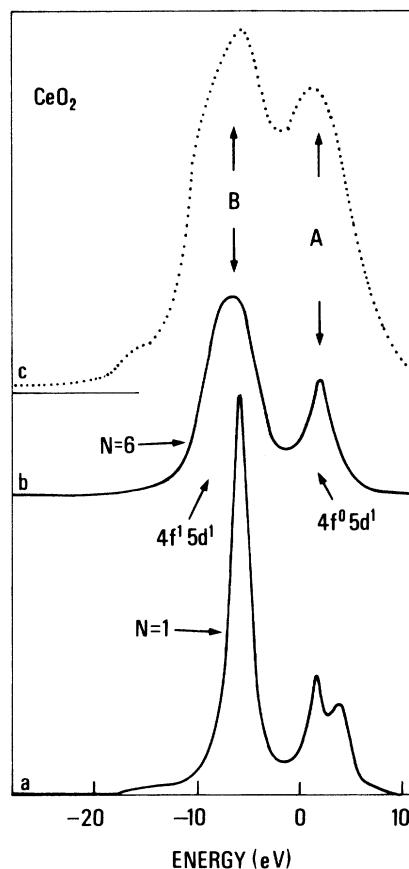


FIG. 3. Calculated core absorption spectra (solid lines) for many-body excitations with a $2p$ core hole and one electron in $5d$ states, in the limit of the molecular cluster ($N=1$, curve a) and in the limit of finite width for filled valence and $5d$ bands ($N=6$, curve b). The theoretical parameters are $U_{df}=5$ eV, $Q_{hf}=-12.5$ eV, $Q_{hd}=-6$ eV, and $\delta\epsilon=1.6$ eV. In the upper part of the figure we report the L_3 absorption edge of CeO_2 after subtraction of an arctan line. After a removal of the arctan curve, which simulates the atomic absorption jump, the structures A and B correspond to transition to the unoccupied d states.

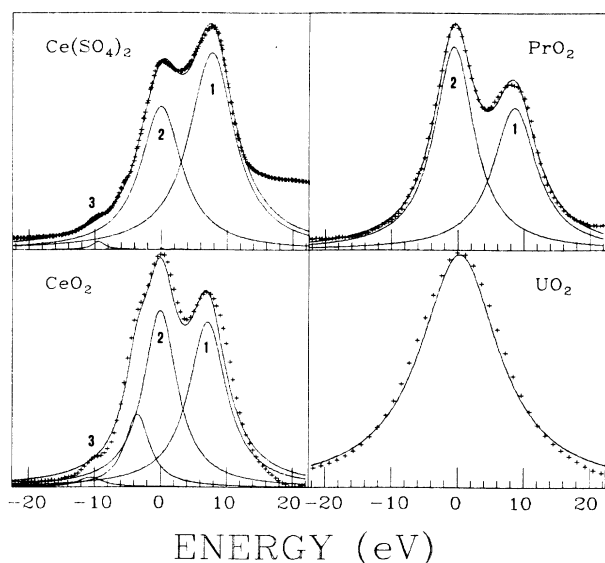


FIG. 4. L_3 absorption threshold of studied samples after subtraction of an arctan curve and the results of fitting with Lorentzians.

materials where the XANES spectra can be fully described by a one-electron model.

The spectra of PrO_2 and cerium sulfate have been analyzed in the same way. The residue of the subtraction of a single arctan curve from the spectrum of CeO_2 in Fig. 2 is reported in Fig. 3 for comparison with theoretical results. The fitting by several Lorentzians of the residues are shown in Fig. 4.

The spectrum of CeO_2 has been fitted with four Lorentzians which, however, are not enough to give account of all details of the line shape of the absorption peaks. Two Lorentzians have been introduced to fit peak B taking account for a shoulder on the low-energy side of peak B . This shoulder is at the energy position of the white line of Ce^{3+} compounds, but $3d$ -XPS spectra of the same CeO_2 sample show no presence of Ce^{3+} ions therefore partial reduction can be excluded. Moreover, on the high-energy side of peak A of the CeO_2 spectrum there is a shoulder that is not fitted with a simple Lorentzian n^01 . Following the theoretical discussion the feature n^01 is determined by $4f^0$ and $4f^2$ final states and feature n^02 by $4f^1$ final state. The peak n^03 is not predicted by the present theory for transitions to d states therefore we assign this last peak to a $2p \rightarrow 6s$ transition.

The usual experimental method to extract the intermediate valence in mixed-valence intermetallics is to fit the L_3 edges with two arctangent and two Lorentzian curves using the same intensity ratio and energy splitting for both curves.^{3-5,30} This procedure is justified where $U_{fd}=0$. In those cases the energy separation between the $4f^n$ and $4f^{n+1}$ x-ray absorption white lines and the XPS core lines are the same but this is not the case for CeO_2 . Where the Coulomb interaction between the photoelectron in a state c in the continuum (above we have studied only the case $c=5d$) and the localized $4f$ electron cannot be disregarded, the energy separation and intensity ratio be-

tween $2p(4f^n)c^1$ and $2p(4f^{n+1}\underline{L})c^1$ final-state configurations for each different state c^1 of the photoelectron at different energies in the XANES are different. Therefore a different energy splitting and different relative intensities of many-body configurations by changing the wave function of the excited photoelectron in the XANES spectrum are expected. Therefore the energy position and the intensity of the second arctangent should be left free in fitting procedure in agreement with the above discussion. We have used this approach but because of the many free parameters several good fittings of the spectra can be obtained with different set of parameters. An alternative fitting procedure, using a minimum number of parameters for these IIV systems, is to neglect the second arctangent and to use the results of Fig. 4. The values of the intermediate valence obtained by this method should be considered as upper limits for the intermediate valence.

Using the standard two Lorentzians and two arctan fitting procedures, we obtain a value of $4f$ occupancy of CeO_2 $x=0.68$ is found (intermediate valence $v=3.32$) and the shoulder B in the CeO_2 spectrum can be fitted with a particular choice of the arctangent in agreement with previous studies.^{3,4} Using the results of the fitting in Fig. 4 we have measured the ratio r between the integrals of the oscillator strength of the experimental features $B/(A+B)$. This has been used to measure the $4f$ number $x=n+r$ (where $n=0,1$, and 2 for Ce, Pr, and U, respectively⁵), because the feature B is pure $4f^1$ and the weight of the $4f^0$ is distributed only on the experimental feature A . The value of r is obtained by the integrals of the Lorentzians of the fitting, where the feature B is given by the sum of the two Lorentzians and we obtain $x=0.54$ for CeO_2 ($v=3.46$). This value of x is smaller than that given by the standard two arctangent, two Lorentzians procedure but is consistent with the band-structure calculations¹³ giving $4f$ occupancy $x=0.47$, with the analysis of the $3d$ XPS spectrum in terms of the many-body configuration-interaction theory $x=0.46$.²⁷

The peaks B and A in the PrO_2 spectrum can be assigned to the $4f^2\underline{L}$ and $4f^1$ configurations, respectively, which are similar to the final-state configurations in CeO_2 . Comparing the spectra of CeO_2 and PrO_2 we can see the effects due to increasing localizations of $4f$ states. Going from CeO_2 to PrO_2 we expect a decrease of the hybridization energy V with increasing localization of $4f$ orbitals and a variation of the energy separation ΔE between the two configurations. We observe a sharpening of B and A features and the experimental spectra can be fitted with only two Lorentzian curves shown in Fig. 4. From Fig. 4 we obtain $x=1.56$ for PrO_2 which is close to the value of $x=1.58$ predicted by Koelling *et al.*¹³

Comparing the spectra of cerium sulfate and CeO_2 we can see the effects due to the different crystal structure for similar local clusters. The sharpening of the A and B features in cerium sulfate is in qualitative agreement with the theoretical predictions shown in Fig. 3 for the decreasing of the dispersion of the O $2p$ band going from CeO_2 to cerium sulfate.

Finally we want to discuss the conditions for interatomic intermediate valence in the ground state. In order to have localized states, U_{ff} should not be negligible, there-

fore the condition $U_{ff} \geq \delta\epsilon$ should be verified. When this condition is satisfied, the mixing between the localized configurations is determined by the hybridization energy V . The intermediate valence is present where $V \sim \Delta E$ on the contrary the integral valence corresponds to $V \ll \Delta E$, where $\Delta E = E(f^{n+1}\underline{L}) - E(f^n)$ is the energy of electron transfer from valence band to the f level with many-body description, i.e., ΔE is the energy difference between f^{n+1} and f^n many-body systems in the limit of vanishing V . The value n is (for nominally tetravalent compounds)

$$n = \begin{cases} 0, & \text{for Ce compounds} \\ 1, & \text{for Pr compounds} \\ 2, & \text{for U compounds} \end{cases}$$

and ΔE is expressed as

$$\Delta E = \begin{cases} \delta\epsilon = \epsilon_f^0 - \epsilon_v^0, & \text{for Ce compounds} \\ \delta\epsilon + U_{ff}, & \text{for Pr compounds} \\ \delta\epsilon + 2U_{ff}, & \text{for U compounds} \end{cases}$$

Here ϵ_v^0 is the center of the valence band, and ϵ_f^0 is the f level in the absence of the f electron interaction U_{ff} .

The intermediate-valence state in CeO_2 and PrO_2 satisfies both conditions $\Delta E \sim V$ and $U_{ff} > \delta\epsilon$. In the case of UO_2 the correlation energy U_{ff} decreases to the value between 2 (Ref. 31) and 4 eV but it is not negligible, therefore we are in the regime $U_{ff} \sim \delta\epsilon$. Because we do not observe splitting of the many-body configuration, the condition $V \ll \Delta E$ should be verified in UO_2 .

CONCLUSION

This experiment has demonstrated that there are insulating correlated systems, like CeO_2 , which exhibit specific ground-state properties in the initial state requiring a many-body picture. These systems are different from the common metallic mixed-valence systems where the Fermi level crosses the single peak of f levels, and there is mix-

ing between $4f^n(5d,6s)^m$ and $4f^{n+1}(5d,6s)^{m-1}$ configurations with energy separation ΔE which can be zero. Insulating interatomic intermediate-valence systems exhibit configuration interaction between f^n and $f^{n+1}\underline{L}$ configurations separated by ΔE (before hybridization). In these systems there is a gap which gives $\Delta E \neq 0$. The hybridization energy V between localized metal and delocalized ligand orbitals and the energy separation ΔE are of the same order of magnitude ($V \sim \Delta E$) (some eV), and the correlation energy satisfies the rule $U_{ff} > \delta\epsilon$.

For these systems the L_3 XANES spectra show multielectron final states and probe directly the ground-state weight of the $f^{n+1}\underline{L}$ configuration. This result is relevant also for the correct interpretation of the saturation of the valence in formally tetravalent intermetallic compounds. In order to obtain the corrected intermediate valence in these IIV systems the contribution of the $f^{n+2}\underline{L}^2$ configuration to the A peak for each system has to be calculated and a careful comparison between all possible final states in core-level spectroscopies K XANES, M XANES, and XPS has to be carried out.

Concerning the recent controversy^{10,11} we have shown that L_3 XANES is a direct probe of configuration interaction in the ground state and therefore a simple one-electron band-structure interpretation of the spectra of IIV systems is not enough because of large- $4f$ correlation energy. The local metal-ligand bonding plays a key role in the determination of the IIV properties as deduced from the comparison between CeO_2 and cerium sulfate. The dispersion of the ligand-derived valence band induces a broadening of the $f^{n+1}\underline{L}$ configuration and a change of hybridization.

Finally we have shown that in UO_2 , where the U_{ff} correlation energy decreases, such that $U_{ff} \sim \delta\epsilon$ and $V \ll \Delta E$, the absorption spectra do not exhibit many-body intermediate-valence effects.

ACKNOWLEDGMENTS

The present paper was prepared when one of the authors (A.K.) was at the Università di Roma "La Sapienza" and he would like to express his thanks to the University of Rome for warm hospitality.

- ¹E. E. Vainsthein, S. Blokhin, and Yu B. Paderno, *Fiz. Tverd. Tela (Leningrad)* **6**, 2909 (1965) [*Sov. Phys.—Solid State* **6**, 2318 (1965)].
- ²P. Burroughs, A. Hamnett, A. F. Orchard, and G. Thornton, *J. Chem. Soc., Dalton Trans.* **17**, 1686 (1976).
- ³G. Krill, J. P. Kappler, A. Meyer, L. Abadli, and M. Ravet, *J. Phys. F* **11**, 1713 (1981).
- ⁴K. R. Bauchspiess, W. Boksich, E. Holland-Moritz, H. Launois, R. Pott, and D. H. Wohlleben, in *Valence Fluctuations in Solids*, edited by L. M. Falicov, W. Hanken, and M. B. Maple (North-Holland, Amsterdam, 1981), p. 417.
- ⁵A. Bianconi, M. Campagna, and S. Stizza, *Phys. Rev. B* **25**, 2477 (1982).
- ⁶A. Bianconi, A. Marcelli, M. Tomellini, and I. Davoli, *J. Magn. Magn. Mater.* **47&48**, 209 (1985).
- ⁷W. Niemann, M. Lubcke, W. Malzfeld, P. Rabe, and R. Haen-

- sel, *J. Magn. Magn. Mater.* **47&48**, 462 (1985).
- ⁸J. Rohler, K. Keulerz, E. Dartyge, A. Fontaine, A. Jucha, and D. Sayers, in *EXAFS and Near Edge Structure*, Vol. 2 of *Springer Proceedings of Physics*, edited by K. Hodgson, B. Hedman, and J. E. Penner-Hahn (Springer-Verlag, Berlin, 1984), p. 385.
- ⁹A. Fujimori, *Phys. Rev. B* **28**, 2281 (1983); **28**, 4489 (1983).
- ¹⁰A. Fujimori, *Phys. Rev. Lett.* **53**, 2518 (1984).
- ¹¹E. Wuilloud, B. Delley, W. D. Schneider, and Y. Baer, *Phys. Rev. Lett.* **53**, 202 (1984); **53**, 2519 (1984).
- ¹²J. L. Smith and P. S. Riseborough, *J. Magn. Magn. Mater.* **47&48**, 545 (1985).
- ¹³D. D. Koelling, A. M. Boering, and J. H. Wood, *Solid State Comm.* **47**, 227 (1983).
- ¹⁴G. Thornton and M. J. Dempsey, *Chem. Phys. Lett.* **77**, 409 (1981).

- ¹⁵V. Heera, G. Seifert, and P. Ziesche, *Phys. Status Solidi B* **118**, K107 (1983); **119**, K1 (1983).
- ¹⁶A. Bianconi, in *X-Ray Absorption: Principles, Applications and Techniques of EXAFS, SEXAFS and XANES*, edited by R. Prinz and D. Konisberger (Wiley, New York, 1986).
- ¹⁷W. Kutzler, K. O. Hodgson, D. Misemer, and S. Doniach, *Chem. Phys. Lett.* **92**, 626 (1982).
- ¹⁸G. Materlik, J. E. Muller, and J. W. Wilkins, *Phys. Rev. Lett.* **50**, 267 (1983).
- ¹⁹C. M. Varma, *Rev. Mod. Phys.* **48**, 219 (1976).
- ²⁰A. Bianconi, A. Marcelli, I. Davoli, S. Stizza, and M. Campagna, *Solid State Commun.* **49**, 409 (1984).
- ²¹G. Calas and J. Petiau, *Solid State Commun.* **54**, 625 (1983).
- ²²P. J. Kelly and M. S. S. Brooks, *J. Phys. C* **13**, L939 (1980).
- ²³Y. Baer and J. Schones, *Solid State Commun.* **54**, 451 (1985).
- ²⁴A. Bianconi, in *EXAFS and Near Edge Structure III*, Vol. 2 of *Springer Proceedings of Physics*, edited by K. O. Hodgson, B. Hedman, and J. Penner-Hahn (Springer-Verlag, Berlin, 1984), p. 167.
- ²⁵A. Kotani and Y. Toyozawa, *J. Phys. Soc. Jpn.* **35**, 1073 (1973); **35**, 1082 (1973); and **37**, 912 (1974).
- ²⁶T. Jo and A. Kotani, *Solid State Commun.* **54**, 451 (1985).
- ²⁷A. Kotani, H. Mizuta, T. Jo, and J. C. Parlebas, *Solid State Commun.* **53**, 805 (1985).
- ²⁸A. Kotani and J. C. Parlebas, *J. Phys. (Paris)* **46**, 77 (1985).
- ²⁹B. Delley and H. Beck, *J. Magn. Magn. Mater.* **47&48**, 269 (1985).
- ³⁰A. Bianconi, S. Modesti, M. Campagna, K. Fisher, and S. Stizza, *J. Phys. C* **14**, 4737 (1981).
- ³¹J. F. Herbst, R. E. Watson, and I. Lingren, *Phys. Rev. B* **14**, 3265 (1986).